

Characterisation of the p53 pathway in cell lines established from TH-MYCN transgenic mouse tumours

Lindi Chen¹, Arman Esfandiari², William Reaves¹, Annette Vu³, Michael D. Hogarty³, John Lunec² and Deborah A. Tweddle^{1*}

¹Wolfson Childhood Cancer Research Centre, Northern Institute for Cancer Research, Newcastle University, Newcastle upon Tyne, United Kingdom.

²Newcastle Cancer Centre, Northern Institute for Cancer Research, Newcastle University, Newcastle upon Tyne, United Kingdom.

³The Children's Hospital of Philadelphia, Perelman School of Medicine, University of Pennsylvania, Philadelphia, Pennsylvania, United States of America.

*Corresponding author. Wolfson Childhood Cancer Research Centre, Northern Institute for Cancer Research, Newcastle University, Level 6 Herschel Building, Brewery Lane, Newcastle upon Tyne, NE1 7RU, United Kingdom. Tel: +44(0)1912082230. Fax: +44(0)1912084301. Email: deborah.tweddle@ncl.ac.uk

Running title: The p53 pathway in TH-MYCN cell lines

Key words: Neuroblastoma; TH-MYCN; p53 pathway; MDM2 inhibitors; Nutlin-3; RG7388; MI-63; NDD0005

Abbreviations:

Ionising radiation (IR)

Wild-type (wt)

Fetal calf serum (FCS)

Abstract

Cell lines established from the TH-MYCN transgenic murine model of neuroblastoma are a valuable preclinical, immunocompetent, syngeneic model of neuroblastoma, for which knowledge of their p53 pathway status is important. *Trp53* status and functional response to Nutlin-3 and ionising radiation (IR) were determined in 6 adherent TH-MYCN transgenic cell lines using Sanger sequencing, immunoblotting and flow cytometry. Sensitivity to structurally diverse MDM2 inhibitors (Nutlin-3, MI-63, RG7388 and NDD0005) were determined using XTT proliferations assays. 2/6 cell lines were *Trp53* homozygous mutant (NHO2A and

844^{MYCN^{+/+}}) and 1/6 (282^{MYCN^{+/-}}) was *Trp53* heterozygous mutant. For 1/6 cell lines (NHO2A), DNA from the corresponding primary tumour was found to be *Trp53* wt. In all cases, the presence of a mutation was consistent with aberrant p53 signalling in response to Nutlin-3 and IR. In comparison to *TP53* wt human neuroblastoma cells, *Trp53* wt murine control and TH-*MYCN* cell lines were significantly less sensitive to growth inhibition mediated by MI-63 and RG7388. These murine *Trp53* wt and mutant TH-*MYCN* cell lines are useful syngeneic immunocompetent neuroblastoma models, the former to test p53-dependent therapies in combination with immunotherapies, such as anti-GD2, and the latter as models of chemoresistant relapsed neuroblastoma when aberrations in the p53 pathway are more common. The spontaneous development of *Trp53* mutations in 3 cell lines from TH-*MYCN* mice may have arisen from *MYCN* oncogenic driven and/or *ex-vivo* selection. The identified species-dependent selectivity of MI-63 and RG7388 should be considered when interpreting *in vivo* toxicity studies of MDM2 inhibitors.

Introduction

Neuroblastoma, an embryonal malignancy of the developing sympathetic nervous system, remains one of the most difficult paediatric cancers to cure with less than 50% of high-risk patients being long-term survivors despite intensive multi-modal therapy. *MYCN* amplification occurs in ~50% of high-risk cases, associating with rapid tumour progression and a poor prognosis (1). The role of *MYCN* in neuroblastoma tumorigenesis was demonstrated by the generation of TH-*MYCN* transgenic mice in 1997 through transfer of a construct incorporating human *MYCN* cDNA under the control of the rat tyrosine hydroxylase promoter into the nucleus of fertilised murine oocytes and subsequent integration into genomic DNA (2, 3). The tyrosine hydroxylase promoter leads to tissue-targeted overexpression of human *MYCN* to neural crest cells, and mice develop spontaneous highly penetrant abdominal and para-spinal thoracic tumours consistent with the sites of human neuroblastoma (2). Tumour penetrance and growth have been shown to be related to *MYCN* gene dosage where homozygotes developed tumours with increased incidence and decreased latency (2, 4). Analysis of the TH-*MYCN* tumours show that they recapitulate many histological features of human neuroblastoma with varying degrees of neuronal differentiation and expression of synaptophysin and neuron-specific enolase (2). Moreover, tumours also exhibit chromosomal changes syntenic with those observed in human neuroblastoma tumours such as gain of chromosome 17 (2, 4). The TH-*MYCN* transgenic mouse is now a well-established model of neuroblastoma, and a panel of homozygous and hemizygous TH-*MYCN* cell lines have been derived from tumour resections

from these mice, similarly reflecting both the genetic and biological features of human neuroblastoma (5). Although micrometastases can occur, one major limitation of the TH-*MYCN* transgenic model in preclinical drug development studies is the very low incidence of clinically relevant metastases to sites such as bone marrow, thus limiting its usefulness as a model for high-risk metastatic neuroblastoma (6). To overcome this, TH-*MYCN* cell lines have been used to generate highly valuable orthotopic and pseudometastatic syngeneic models of neuroblastoma in an immunoprecient background (7, 8). This is particularly important as immunotherapies such as anti-GD2 antibody are now standard of care for treatment of children with high-risk neuroblastoma.

The tumour suppressor gene *TP53* is critical in maintaining genomic stability and is mutationally inactivated in >50% of all human malignancies (9). Abnormalities in the p53 pathway can contribute to tumour resistance against ionising radiation (IR) and cytotoxic chemotherapies (10-13). In neuroblastoma tumours and cell lines established at diagnosis, *TP53* mutations are rare however an increased frequency of mutations have been reported at relapse/post-chemotherapy (14-16). Knowledge of *Trp53* genetic and functional status in TH-*MYCN* cell lines is important if they are to be used in preclinical syngeneic neuroblastoma models.

Here we characterised the genetic and functional status of p53 in 6 adherent TH-*MYCN* transgenic murine cell lines, and demonstrate that 3/6 cell lines have *Trp53* mutations and could be used to generate valuable syngeneic models of p53 non-functional relapsed neuroblastoma. Moreover, we provide evidence of species-dependent selectivity of selected MDM2 inhibitors, which should be considered when selecting murine models for preclinical toxicity testing of MDM2 inhibitors.

Materials and methods

Cell lines

TH-*MYCN* transgenic murine cell lines used were *MYCN* homozygous NHO2A, 844^{*MYCN*+/+}, 3261^{*MYCN*+/+}, 3394^{*MYCN*+/+}, 3399^{*MYCN*+/+} and hemizygous 282^{*MYCN*+/-}. NHO2A has been previously described (5) and together with NHO2A mouse tumour DNA were obtained from Michelle Haber (Children's Cancer Institute, Sydney, Australia). All other previously unreported TH-*MYCN* cell lines were established from the TH-*MYCN* colony at the Children's Hospital of Philadelphia under an IACUC approved animal protocol. Tumour-bearing mice were euthanized according to humane approved guidelines using isoflurane inhalation followed

by cervical dislocation and disinfected with 70% ethanol prior to dissecting the tumour free. Tumours were fragmented and filtered through a 40 µm nylon mesh filter into a conical tube, spun-pelleted, and resuspended in sterile Tris Ammonia Chloride buffer, buffered to pH 7.65. Tumour cell pellets were incubated at 37 C for 5 minutes, rinsed and spun-pelleted multiple times in PBS and then plated in RPMI tissue culture media supplemented with 10% FBS, 1% L-glutamin and 1% Penicillin/Streptomycin/Gentamycin. Cells were propagated under routine tissue culture conditions and ~50% result in an established cell line over ~8 weeks. The TH-*MYCN* cell lines established were validated as tyrosine hydroxylase positive by RT-PCR (>95%+) and have surface expression of the GD2 disialoganglioside detected by flow-cytometry. Control murine cell lines used were *Trp53* wild-type (wt) MEF^{PARP^{-/-}} obtained from Gilbert de Murcia (17) and NIH3T3 cells. Control human neuroblastoma cell lines used were *TP53* mutant, *MYCN* amplified SKnBe2C and *TP53* wt non-*MYCN* amplified SHSY5Y (obtained from Penny Lovat (Newcastle University) and June Biedler (Memorial Sloan Kettering) and authenticated by multiplex short tandem repeat profiling by NewGene Limited (Newcastle upon Tyne, UK) using GenePrint® 10 System) and *TP53* wt *MYCN*-amplified NGP cells (18). NHO2A cells were cultured as previously described (5). 844^{MYCN^{+/+}}, 282^{MYCN^{+/-}}, SHSY5Y, SKnBe2C and NGP cells were cultured in RPMI-1640 (Sigma-Aldrich, UK) supplemented with 10% fetal calf serum (FCS) (Gibco, Paisley, Scotland), and 3261^{MYCN^{+/+}}, 3394^{MYCN^{+/+}} and 3399^{MYCN^{+/+}} cells were cultured in RPMI-1640 supplemented with 20% FCS. MEF^{PARP^{-/-}} and NIH3T3 cells were cultured in Dulbecco's Modified Eagle's Medium (Sigma-Aldrich) supplemented with 10% FCS.

***Trp53* sequencing**

DNA was extracted from tumour and cell lines using a DNeasy Blood & Tissue Kit (Qiagen, Manchester, UK) according to the manufacturer's protocol. DNA from NHO2A, 844^{MYCN^{+/+}} and 282^{MYCN^{+/-}} was amplified for *Trp53* exons 2-10 and sequenced in both directions by DBS genomics (Durham University, UK). Primer sequences available on request. 3261^{MYCN^{+/+}}, 3394^{MYCN^{+/+}}, and 3399^{MYCN^{+/+}} DNA samples were amplified and sequenced in both directions for *Trp53* exons 5-10 by LGC Genomics GmbH (Berlin, Germany).

MDM2 inhibitors, IR, immunoblotting and flow cytometry

MDM2 inhibitors Nutlin-3, MI-63, NDD0005 and RG7388 were obtained, and growth inhibition assays, immunoblotting and flow cytometry performed as previously described (19, 20). Cells were irradiated using a RS320 irradiator (Gulmay Medical, Surrey, UK). Primary

antibodies used were p53 1:1000 (CM5; Leica Microsystems Ltd, UK), MYCN 1:100 (NCMII00; Merck Millipore, Billerica, MA), p21^{WAF1} 1:1000 (SX118; BD), MDM2 1:500 (2A10; Abcam, Cambridge, MA), p19^{ARF} 1:500 (ab80; Abcam) and GAPDH 1:500 (FL335; Santa Cruz Biotechnology, Inc., Dallas, TX).

Statistical analyses

Two-sided unpaired t-tests were performed using GraphPad Prism v6.0 software with $P < 0.05$ taken as the level of significance.

Results

Trp53 status of TH-MYCN cell lines

All TH-MYCN transgenic cell lines used in the present study were cultured as adherent monolayers (Figure 1A). *Trp53* Sanger sequencing identified that 3/6 cell lines, NHO2A, 844^{MYCN+/+} and 282^{MYCN+/-}, had missense coding region point mutations (Figure 1B-D). NHO2A cells were homozygous for a p.F106S (phenylalanine to serine; c.317 C>T) *Trp53* mutation corresponding to the human p.F109S *TP53* missense mutation (Figure 1B). 844^{MYCN+/+} were *Trp53* homozygous mutant for a p.C173W (cysteine to tryptophan; c.519 C>G) mutation corresponding to the human p.C176W missense mutation (Figure 1C). Interestingly, 282^{MYCN+/-} were heterozygously mutated for the same *Trp53* p.C173W mutant allele as 844^{MYCN+/+} cells (Figure 1D). Both p.F106S and p.C173W mutations are within the DNA binding domain and shown to affect p53 mediated transactivation using the TP53Mutload Database. The homozygous mutations detected in NHO2A and 844^{MYCN+/+} cells are most likely due to be due to allelic loss of one allele with mutation in the remaining allele.

To determine whether the mutations present in cell lines were also present in the original tumours or selected for during the establishment of the cell line, tumour DNA was sequenced for *Trp53* exons 2-10. Only 1/6 cell lines (NHO2A) had tumour DNA available and was found to be wt (Figure 1E).

MYCN and the p53 pathway in TH-MYCN cell lines

Basal expression of MYCN and p53 pathway components, namely p53, MDM2, p21^{WAF1} and p19^{ARF} were assessed in TH-MYCN cell lines using Western blotting (Figure 1F). *Trp53* wt murine MEF^{PARP-/-} and NIH3T3, and human MYCN amplified *TP53* mutant SKnBe2C cells were included as controls. Overexpression of the MYCN transgene was observed in all TH-MYCN cell lines, with levels comparable to MYCN amplified SKNBe2C cells. NHO2A

and 844^{MYCN^{+/+}} had the highest MYCN levels compared to other TH-MYCN cell lines. Accumulation of p53 was observed in NHO2A, 844^{MYCN^{+/+}} and 282^{MYCN^{+/-}} cells consistent with their mutant *Trp53* status. All mouse cell lines had very low or undetectable baseline MDM2 expression (Figure 1F). p21^{WAF1} was expressed only in the *Trp53* wt 3399^{MYCN^{+/+}} cell line (Figure 1F). p19^{ARF} was expressed in NHO2A, 844^{MYCN^{+/+}}, 3394^{MYCN^{+/+}} and 3399^{MYCN^{+/+}} cells (Figure 1F).

The p53 pathway response to Nutlin-3 and IR

Using Nutlin-3 and IR as different methods to induce p53 activation, the p53 signalling pathway was assessed by Western blotting in the TH-MYCN cell lines and the control *Trp53* wt MEF^{PARP^{-/-}} cells (Figures 2&3). Consistent with their *Trp53* wt status, MEF^{PARP^{-/-}} cells showed an intact p53 signalling pathway in response to both Nutlin-3 and IR, evident by p53 stabilisation and MDM2 and p21^{WAF1} upregulation (Figure 2A&3A). Interestingly, the p53 pathway response of MEF^{PARP^{-/-}} cells to IR was slightly diminished and delayed in comparison to Nutlin-3 (Figure 2A&3A), and is most likely a consequence of *PARP-1* knockout in this cell line (21). As expected, homozygously *Trp53* mutant NHO2A and 844^{MYCN^{+/+}} cells failed to show p53 induction in response to Nutlin-3 (Figure 2B & C) or IR (Figure 3B & C). Consistent with this, no p21^{WAF1} induction was observed in either cell line, or MDM2 in 844^{MYCN^{+/+}} cells. Interestingly, despite a lack of p53 induction, weak induction of MDM2 was observed in NHO2A cells after both Nutlin-3 treatment and IR (Figures 2B & 3B). Heterozygously *Trp53* mutant 282^{MYCN^{+/-}} cells also failed to show p53 stabilisation in response to Nutlin-3 or IR, however despite this, an increase in both MDM2 and p21^{WAF1} expression was observed (Figures 2D & 3D), most likely as a result of the presence of one remaining wt *Trp53* allele. Finally, in line with their *Trp53* wt status the 3 remaining TH-MYCN cell lines, 3261^{MYCN^{+/+}}, 3394^{MYCN^{+/+}} and 3399^{MYCN^{+/+}} all showed evidence of IR and Nutlin-3 induced p53 pathway activation, with stabilisation of p53 and induction of p21 and MDM2 (Figure 2E-G and 3E-G).

Nutlin-3 induced cell cycle distribution

To further characterise the p53 functional response in TH-MYCN cell lines to Nutlin-3, the sub-G₁ and cell cycle distribution of all 6 TH-MYCN cell lines following 24 hours of 20 μM Nutlin-3 treatment were analysed by propidium iodide based flow cytometry. Sub-G₁ events was used as a surrogate marker of apoptosis and the G₁:S ratio calculated as an indicator of G₁ cell cycle arrest. *Trp53* wt NIH3T3 and MEF^{PARP^{-/-}} were included as positive controls. Functional assessment of Nutlin-3 mediated cell cycle arrest and apoptosis in human

neuroblastoma cell lines have previously been reported (22, 23). In response to Nutlin-3 treatment, NIH3T3 cells underwent a G₁ arrest, evident by a 4.6-fold increase in their G₁/S ratio (16.58±4.43 (Nutlin-3) versus 3.61 ± 0.17 (DMSO); Table 1 & Figure 4A). Consistent with the observed activation of the p53 pathway in Figure 2A, the MEF^{PARP^{-/-}} cells demonstrated a 3.2-fold increase in their G₁:S ratio (7.19 ± 3.32 (Nutlin-3) versus 2.23 ± 0.23 (DMSO)), and a significant increase in the percentage of cells in G₂/M (53.32% ± 4.19 (Nutlin-3) versus 34.75% ± 1.63 (DMSO); *P*<0.005, paired *t*-test) (Table 1 & Figure 4A), indicative of a Nutlin-3 induced G₁ and particularly G₂ arrest in this cell line. In contrast to control *Trp53* wt murine cell lines and as expected, no change in G₁/S ratio or percentage of cells in G₂/M were observed in any *Trp53* mutant TH-*MYCN* NHO2A, 844^{MYCN^{+/+}} or 282^{MYCN^{+/-}} cells (Table 1 & Figure 4A). Interestingly, compared to other murine cell lines, NHO2A and 282^{MYCN^{+/-}} cells had a high proportion of sub-G₁ basal events (Table 1 & Figure 4A), a surrogate marker of apoptosis, which following Nutlin-3 treatment increased slightly and remained unchanged, respectively. Consistent with their *Trp53* wt status and observed p53 pathway activation in Figure 2E-G, the 3 *Trp53* wt TH-*MYCN* cell lines, 3261^{MYCN^{+/+}}, 3394^{MYCN^{+/+}} and 3399^{MYCN^{+/+}} all underwent a G₁ arrest evident by a 5.2-, 5- and 3.4-fold increase in G₁/S ratio compared to control cells, respectively (Table 1 & Figure 4A). In addition, 3399^{MYCN^{+/+}} cells also exhibited an increased sub-G₁ population (Table 1 & Figure 4A).

Species-dependent MDM2 inhibitor selectivity

MDM2 inhibitors are currently under preclinical and clinical evaluation as a novel therapeutic for neuroblastoma. To further evaluate the p53 pathway status of cell lines studied and establish their response to MDM2 inhibitors, sensitivity to Nutlin-3 and additional structurally unrelated MDM2 inhibitors, NDD0005, MI-63 and RG7388 mediated growth inhibition were assessed (Table 2). Human *TP53* wt non-*MYCN* amplified SHSY5Y and *MYCN* amplified NGP cells which have previously been shown to be sensitive to the tested MDM2 inhibitors were included as positive controls (19, 20, 22). The concentrations of Nutlin-3, MI63, NDD0005 and RG7388 which led to 50% growth inhibition (GI₅₀) after 48 hours of treatment are shown in Table 2. In comparison to *TP53* wt human neuroblastoma cells, *Trp53* wt control and TH-*MYCN* murine cell lines were less sensitive to Nutlin-3 mediated growth inhibition as evident by higher GI₅₀ concentrations (1.2-7.4 fold less sensitive; Table 2 & Figure 4B). As expected, *Trp53* mutant TH-*MYCN* cell lines NHO2A, 844^{MYCN^{+/+}} and 282^{MYCN^{+/-}} had the highest GI₅₀ values (14.1-21.8 fold less sensitive, Table 2).

Further evaluation and comparison of *Trp53* wt TH-*MYCN* and *MEF^{PARP-/-}* cells to NDD0005, MI-63 and RG7388, demonstrated that although *MEF^{PARP-/-}* cells were significantly (2.5-3.6 fold) less sensitive to NDD0005, there was no difference in the sensitivity of *Trp53* wt TH-*MYCN* cell lines to NDD0005 compared with human SHSY5Y and NGP neuroblastoma cells (Table 2 & Figure 4C). Of the tested MDM2 inhibitors, MI-63 and RG7388 were the most potent against the human neuroblastoma cell lines, consistent with our previous studies (19, 22). The data also revealed that compared with SHSY5Y and NGP cells, *Trp53* wt *MEF^{PARP-/-}* cells were significantly (11.3-15.4 and 11.9-15.0 fold) less sensitive to both MI-63 and RG7388, respectively (Table 2; Figure 4D & E). Furthermore, the data also show that *Trp53* wt TH-*MYCN* cell lines were significantly (3.5-5.1 fold) less sensitive to MI-63 (Table 2 & Figure 4D), and even less so (13.6-59.1 fold) to RG7388 (Table 2 & Figure 4E). This highlights an inverse relationship between potency in *TP53* wt human neuroblastoma cells and potency in *Trp53* wt murine cells.

Discussion

Cell lines established from primary tumours resected from TH-*MYCN* mice have been used to develop valuable preclinical immunocompetent, syngeneic models of neuroblastoma (7, 8), for which knowledge of their p53 pathway status is important. Here we show that 2/6 TH-*MYCN* cell lines were *Trp53* homozygous mutant (NHO2A and 844^{*MYCN*+/+}) and 1/6 was heterozygous mutant (282^{*MYCN*+/-}). In the only case where DNA from the original tumour was available (NHO2A), the original tumour was *Trp53* wt. This is consistent with our previous analysis of 13 primary TH-*MYCN* tumours which did not show any *Trp53* mutations (exons 4-8) (24). It is possible that *Trp53* mutant subpopulations existed within the primary tumour but were too small and below the level of detection of Sanger sequencing or that the mutation spontaneously developed and was selected for during *ex-vivo* culturing pressures and cell line establishment. A *MYCN* oncogenic drive may be a strong contributing factor for the positive selection of *Trp53* mutations and may account for why 3/6 TH-*MYCN* cell lines tested in the present study were either homozygous or heterozygous *Trp53* mutant. Certainly, *MYCN* is known to play a dual role in driving both proliferation and apoptosis, and there are several lines of evidence, including studies using TH-*MYCN* models, which suggest that *MYCN* driven p53-dependent apoptosis is an important mechanism for tumour suppression in neuroblastoma and that *MYCN* amplified neuroblastoma cells may circumvent *MYCN* driven p53-dependent apoptosis by selecting for cells with aberrations in the p53/MDM2/p14^{ARF} pathway, as is seen for MYCC-driven lymphoma (3, 18, 25-28). Specifically, tumours formed with greater

penetrance and reduced latency in TH-*MYCN* mice heterozygous for an inactivated germline p53 allele (26). Analysis of human neuroblastoma cell lines reported to date with aberrations in the p53/MDM2/p14^{ARF} pathway demonstrates that 31/40 (78%) are *MYCN* amplified (18). More recently, a study of the role of p53 function in neuroblastoma pathogenesis using TH-*MYCN* murine models observed that loss of p53 function led to reduced survival (29).

Nutlin-3 is a potent selective inhibitor of the MDM2-p53 interaction (30), previously shown to be highly effective against *TP53* wt neuroblastoma cell lines, inducing cell cycle arrest and/or apoptosis, and used to functionally screen large neuroblastoma cell line panels for p53 pathway aberrations (22, 23, 31). We found that in all cell lines tested, the presence of a mutation was consistent with high basal levels of p53 and aberrant p53 signalling in response to Nutlin-3 and IR, and failure to growth arrest in response to Nutlin-3. Consistent with the mechanism of action of MDM2 inhibitors and existing data from human neuroblastoma cell lines, overall Nutlin-3 was found to induce a cell cycle arrest and/or apoptosis in *Trp53* wt control and TH-*MYCN* murine cell lines (22, 23). Interestingly in the current study, in response to Nutlin-3 and IR, although there was no induction of p53, an increase in both MDM2 and p21^{WAF1} expression was observed in the heterozygously mutant 282^{*MYCN*+/-} cells, suggesting that there is some residual p53 function from the remaining wt allele (32), however this did not lead to a growth arrest or apoptosis in response to Nutlin-3.

MDM2 inhibitors are currently under preclinical and clinical development as a novel therapeutic, both alone and in combination, for human malignancies including neuroblastoma. Of particular interest in view of the latter, data from the present study has demonstrated that in comparison to human *TP53* wt neuroblastoma cells, murine control (*MEF^{PARP-/-}*) and TH-*MYCN* cell lines were significantly less sensitive to MI-63 and RG7388 induced growth inhibition. Although human and murine MDM2 show a high degree of amino acid sequence homology, with only 2 non-identical amino acids within the p53 binding domain (33), these subtle differences could account for a weaker binding affinity to murine MDM2 which is believed to contribute to the increased resistance and higher GI₅₀ concentrations of murine cells to some MDM2 inhibitors that have been designed with high potency against human MDM2 (34). In support of this, the present data shows that the more potent the MDM2 inhibitor is against human neuroblastoma cells, the less sensitive the murine cells are, and the greater the fold difference between GI₅₀ values of *Trp53* wt murine cells versus *TP53* wt human cells. These observations are consistent with the inter-species selectivity of spiro-oxindole-based MDM2 inhibitors (35) and dihydroisoquinolinone NVP-CGM097 (36) but not

pyrazolopyrrolidinone NVP-HDM201 (37, 38), and should be taken into account when designing studies of MDM2 inhibitors either alone or in combination using either preclinical transgenic or human tumour xenograft models as p53-dependent normal tissue toxicity will not be adequately modelled.

Currently, murine neuroblastoma models include genetically engineered mouse models, syngeneic models, and subcutaneous, orthotopic, pseudometastatic and patient-derived xenografts (3, 39-42). All models have associated advantages and disadvantages, and it is likely that the most comprehensive preclinical assessment of efficacy will include a combination of existing models. Several of the models predominantly use immunocompromised mice and thus are unsuitable for the assessment of immunotherapies, which are emerging as effective targeted therapies in patients with neuroblastoma. To overcome this, cell lines established from the TH-*MYCN* transgenic model/or other murine neuroblastoma cell lines can be used to generate orthotopic or pseudometastatic syngeneic models of neuroblastoma in an immunocompetent background (7, 8). For this, the genetic and functional characterisation of murine cell lines, including *Trp53* status and pathway function, are very important and highly warranted, and existing data are limited. In conclusion, the *Trp53* wt and mutant TH-*MYCN* cell lines characterised in this study can be used in highly valuable and needed syngeneic models of neuroblastoma, the former to test p53-dependent therapies in combination with immunotherapies, such as anti-GD2 antibody, and the latter as models of immunocompetent, chemoresistant relapsed neuroblastoma in which aberrations in the p53 pathway are more common (14-16).

Acknowledgments

This work was supported by The Dubois Cancer Fund, SPARKS, the North of England Children's Cancer Fund (NECCRF), Neuroblastoma UK and Niamh's Next Step. We would like to thank Michelle Haber for the NHO2A cell line and tumour DNA, Gilbert de Murcia for providing MEF^{PARP^{-/-}} cells, Fabio Del Bello and Alessandro Piergentili for providing MI-63, Steven Middleton (Roche-Genentech) for providing RG7388, and Anna Watson, Karen Haggerty and Ian Hardcastle (Newcastle University) for synthesising NDD0005.

Conflict of interest statement

We disclose that L. Chen and D.A. Tweddle are part of an international collaborative research consortium with Hoffmann-La Roche Ltd. J. Lunec is a collaborative co-investigator of the CRUK funded Drug Discovery Programme at Newcastle University which developed

NDD0005. Newcastle University, Cancer Research Technology and Astex Pharmaceuticals Inc. are part of an alliance agreement since 2012.

References

1. Cohn SL and Tweddle DA: MYCN amplification remains prognostically strong 20 years after its "clinical debut". *Eur J Cancer* 40: 2639-2642, 2004.
2. Weiss WA, Aldape K, Mohapatra G, Feuerstein BG and Bishop JM: Targeted expression of MYCN causes neuroblastoma in transgenic mice. *EMBO J* 16: 2985-2995, 1997.
3. Chesler L and Weiss WA: Genetically engineered murine models--contribution to our understanding of the genetics, molecular pathology and therapeutic targeting of neuroblastoma. *Seminars in cancer biology* 21: 245-255, 2011.
4. Rasmuson A, Segerstrom L, Nethander M, et al.: Tumor development, growth characteristics and spectrum of genetic aberrations in the TH-MYCN mouse model of neuroblastoma. *PloS one* 7: e51297, 2012.
5. Cheng AJ, Ching Cheng N, Ford J, et al.: Cell lines from MYCN transgenic murine tumours reflect the molecular and biological characteristics of human neuroblastoma. *European Journal of Cancer* 43: 1467-1475, 2007.
6. Lehembre F and Regenass U: Metastatic disease: A drug discovery perspective. *Seminars in Cancer Biology* 22: 261-271, 2012.
7. Stauffer JK, Orentas RJ, Lincoln E, et al.: High-throughput molecular and histopathologic profiling of tumor tissue in a novel transplantable model of murine neuroblastoma: new tools for pediatric drug discovery. *Cancer investigation* 30: 343-363, 2012.
8. Kroesen M, Nierkens S, Ansems M, et al.: A transplantable TH-MYCN transgenic tumor model in C57Bl/6 mice for preclinical immunological studies in neuroblastoma. *International journal of cancer* 134: 1335-1345, 2014.
9. Brown CJ, Lain S, Verma CS, Fersht AR and Lane DP: Awakening guardian angels: drugging the p53 pathway. *Nature reviews* 9: 862-873, 2009.
10. Carr J, Bell E, Pearson ADJ, et al.: Increased Frequency of Aberrations in the p53/MDM2/p14ARF Pathway in Neuroblastoma Cell Lines Established at Relapse. *Cancer Research* 66: 2138-2145, 2006.
11. Keshelava N, Zuo JJ, Chen P, et al.: Loss of p53 Function Confers High-Level Multidrug Resistance in Neuroblastoma Cell Lines. *Cancer Research* 61: 6185-6193, 2001.
12. Levine AJ: p53, the Cellular Gatekeeper for Growth and Division. *Cell* 88: 323-331, 1997.
13. Soussi T and Beroud C: Assessing TP53 status in human tumours to evaluate clinical outcome. *Nat Rev Cancer* 1: 233-239, 2001.
14. Carr-Wilkinson J, O'Toole K, Wood KM, et al.: High Frequency of p53/MDM2/p14ARF Pathway Abnormalities in Relapsed Neuroblastoma. *Clin Cancer Res* 16: 1108-1118, 2010.
15. Tweddle DA, Malcolm AJ, Bown N, Pearson AD and Lunec J: Evidence for the development of p53 mutations after cytotoxic therapy in a neuroblastoma cell line. *Cancer research* 61: 8-13, 2001.
16. Padovan-Merhar OM, Raman P, Ostrovnya I, et al.: Enrichment of Targetable Mutations in the Relapsed Neuroblastoma Genome. *PLoS Genet* 12: e1006501, 2016.
17. de Murcia JM, Niedergang C, Trucco C, et al.: Requirement of poly(ADP-ribose) polymerase in recovery from DNA damage in mice and in cells. *Proc Natl Acad Sci U S A* 94: 7303-7307, 1997.
18. Chen L and Tweddle DA: p53, SKP2, and DKK3 as MYCN Target Genes and Their Potential Therapeutic Significance. *Frontiers in oncology* 2: 173, 2012.

19. Chen L, Zhao Y, Halliday GC, et al.: Structurally diverse MDM2-p53 antagonists act as modulators of MDR-1 function in neuroblastoma. *British journal of cancer* 111: 716-725, 2014.
20. Chen L, Rousseau RF, Middleton SA, et al.: Pre-clinical evaluation of the MDM2-p53 antagonist RG7388 alone and in combination with chemotherapy in neuroblastoma. *Oncotarget* 6: 10207-10221, 2015.
21. Valenzuela MT, Guerrero R, Nunez MI, et al.: PARP-1 modifies the effectiveness of p53-mediated DNA damage response. *Oncogene* 21: 1108-1116, 2002.
22. Gamble LD, Kees UR, Tweddle DA and Lunec J: MYCN sensitizes neuroblastoma to the MDM2-p53 antagonists Nutlin-3 and MI-63. *Oncogene* 31: 752-763, 2012.
23. Van Maerken T, Rihani A, Dreidax D, et al.: Functional analysis of the p53 pathway in neuroblastoma cells using the small-molecule MDM2 antagonist nutlin-3. *Molecular cancer therapeutics* 10: 983-993, 2011.
24. Mazanek P, Dam V, Morgan BT, Liu X, Pawar N and Hogarty MD: Assessment of p19/ARF-MDM-p53 and RAS pathways for alterations in neuroblastomas arising in the transgenic TH-MYCN mouse model. In: *Advances in Neuroblastoma Research June 16-19th 2004*, , Genoa, Italy, 2004.
25. Chen L, Iraci N, Gherardi S, et al.: p53 Is a Direct Transcriptional Target of MYCN in Neuroblastoma. *Cancer research* 70: 1377-1388, 2010.
26. Chesler L, Goldenberg DD, Collins R, et al.: Chemotherapy-induced apoptosis in a transgenic model of neuroblastoma proceeds through p53 induction. *Neoplasia (New York, N.Y)* 10: 1268-1274, 2008.
27. Chen Z, Lin Y, Barbieri E, et al.: Mdm2 deficiency suppresses MYCN-Driven neuroblastoma tumorigenesis in vivo. *Neoplasia (New York, N.Y)* 11: 753-762, 2009.
28. Eischen CM, Weber JD, Roussel MF, Sherr CJ and Cleveland JL: Disruption of the ARF-Mdm2-p53 tumor suppressor pathway in Myc-induced lymphomagenesis. *Genes Dev* 13: 2658-2669, 1999.
29. Yogev O, Barker K, Sikka A, et al.: p53 Loss in MYC-Driven Neuroblastoma Leads to Metabolic Adaptations Supporting Radioresistance. *Cancer research* 76: 3025-3035, 2016.
30. Vassilev LT, Vu BT, Graves B, et al.: In vivo activation of the p53 pathway by small-molecule antagonists of MDM2. *Science (New York, N.Y)* 303: 844-848, 2004.
31. Chen L, Malcolm AJ, Wood KM, et al.: p53 is nuclear and functional in both undifferentiated and differentiated neuroblastoma. *Cell cycle (Georgetown, Tex)* 6: 2685-2696, 2007.
32. Sun Y, Yi H, Yang Y, et al.: Functional characterization of p53 in nasopharyngeal carcinoma by stable shRNA expression. *International journal of oncology* 34: 1017-1027, 2009.
33. Vassilev LT: Small-molecule antagonists of p53-MDM2 binding: research tools and potential therapeutics. *Cell cycle (Georgetown, Tex)* 3: 419-421, 2004.
34. Khoo KH, Verma CS and Lane DP: Drugging the p53 pathway: understanding the route to clinical efficacy. *Nature reviews. Drug discovery* 13: 217-236, 2014.
35. Delaisi C, Meaux I, Dos-Santos O, et al.: In vitro characterization of spiro-oxindole-based modulators of the MDM2-p53 interaction and their interspecies selectivity. In: *Proceedings of the 103rd Annual Meeting of the American Association for Cancer Research 2012-Mar 31-Apr 4, 2012 Cancer Res 2012;72(8 Suppl):Abstract nr 4648*, Chicago, IL, Philadelphia (PA), 2012.
36. Holzer P, Masuya K, Furet P, et al.: Discovery of a Dihydroisoquinolinone Derivative (NVP-CGM097): A Highly Potent and Selective MDM2 Inhibitor Undergoing Phase 1 Clinical Trials in p53wt Tumors. *Journal of medicinal chemistry* 58: 6348-6358, 2015.

37. Stachyra-Valat T, Baysang F, D'Alessandro A-C, et al.: Abstract 1239: NVP-HDM201: Biochemical and biophysical profile of a novel highly potent and selective PPI inhibitor of p53-Mdm2. *Cancer research* 76: 1239-1239, 2016.
38. Furet P, Masuya K, Kallen J, et al.: Discovery of a novel class of highly potent inhibitors of the p53–MDM2 interaction by structure-based design starting from a conformational argument. *Bioorganic & medicinal chemistry letters* 26: 4837-4841, 2016.
39. Heukamp LC, Thor T, Schramm A, et al.: Targeted expression of mutated ALK induces neuroblastoma in transgenic mice. *Science translational medicine* 4: 141ra191, 2012.
40. Khanna C and Hunter K: Modeling metastasis in vivo. *Carcinogenesis* 26: 513-523, 2005.
41. Khanna C, Jaboin JJ, Drakos E, Tsokos M and Thiele CJ: Biologically relevant orthotopic neuroblastoma xenograft models: primary adrenal tumor growth and spontaneous distant metastasis. *In vivo* 16: 77-85, 2002.
42. Beltinger C and Debatin KM: Murine models for experimental therapy of pediatric solid tumors with poor prognosis. *International journal of cancer* 92: 313-318, 2001.

Figure Legends

Figure 1. A) Photomicrographs showing the morphological appearance of NHO2A, 282^{MYCN+/-}, 844^{MYCN+/+}, 3261^{MYCN+/+}, 3394^{MYCN+/+} and 3399^{MYCN+/+} TH-MYCN murine neuroblastoma cell lines. Chromatograms showing *Trp53* gene mutations identified in B) NHO2A (homozygous mutation, codon 106, Phenylalanine to Serine), C) 844^{MYCN+/+} (homozygous mutation, codon 173, Cysteine to Tryptophan) and D) 282^{MYCN+/-} (heterozygous mutation, codon 173, Cysteine to Tryptophan). All mutations are within the DNA binding domain of p53. *marks the nucleotide change. E) Chromatograms showing the *Trp53* wt status of the original tumour from which the NHO2A cell line was derived compared to the homozygous p.F106S (c.317C>T) mutation identified in the NHO2A cell line. F) Western analysis of basal expression of MYCN, MDM2, p53, p21^{WAF1} and p19^{ARF} (murine homologue of p14^{ARF}) in the murine cell line panel in comparison to the *TP53* mutant *MYCN* amplified SKNBe2C human neuroblastoma cell line. *p53 and p19^{ARF} antibodies are only reactive against murine p53 and p19^{ARF}.

Figure 2. The p53 pathway response of MEF^{PARP-/-} and TH-MYCN transgenic murine cell lines to the MDM2 inhibitor, Nutlin-3. Western analysis showing the levels of p53 and p53 target genes, MDM2 and p21^{WAF1} in A) MEF^{PARP-/-}, B) NHO2A, C) 844^{MYCN+/+}, D) 282^{MYCN+/-}, E) 3261^{MYCN+/+}, F) 3394^{MYCN+/+} and G) 3399^{MYCN+/+} cells after 6, 24 and 48 h 20μM Nutlin-3 treatment. Control cells were treated with either media alone (M) or media containing an equal volume of DMSO (DMSO).

Figure 3. The p53 pathway response of MEF^{PARP-/-} and TH-MYCN transgenic murine cell lines to IR induced DNA damage. Western analysis showing the levels of p53 and p53 target genes, MDM2 and A) MEF^{PARP-/-}, B) NHO2A, C) 844^{MYCN+/+}, D) 282^{MYCN+/-}, E) 3261^{MYCN+/+}, F)

3394^{MYCN^{+/+}} and G) 3399^{MYCN^{+/+}} cells at 6, 24 and 48 h after 10Gy IR. Control cells received no IR (M).

Figure 4. Cell cycle distribution and sensitivity of murine cell lines in response to Nutlin-3. A) Graph showing the cell cycle distribution of *Trp53* wt murine control cells NIH3T3 and MEF^{PARP^{-/-}}, and the 6 TH-*MYCN* cell lines after 24 h treatment with 20 μM Nutlin-3. Control cells were treated with media containing an equal volume of DMSO (DMSO). Error bars represent the SEM for n=3 repeat experiments. wt, *Trp53* wt; mut, *Trp53* mutant. Dose-response growth inhibition curves for p53 wt human SHSY5Y and NGP, murine MEF^{PARP^{-/-}} and TH-*MYCN* 3261^{MYCN^{+/+}}, 3394^{MYCN^{+/+}} and 3399^{MYCN^{+/+}} cells in response to 48 h treatment with B) Nutlin-3, C) NDD0005, D) MI-63 and E) RG7388.

Figure 1

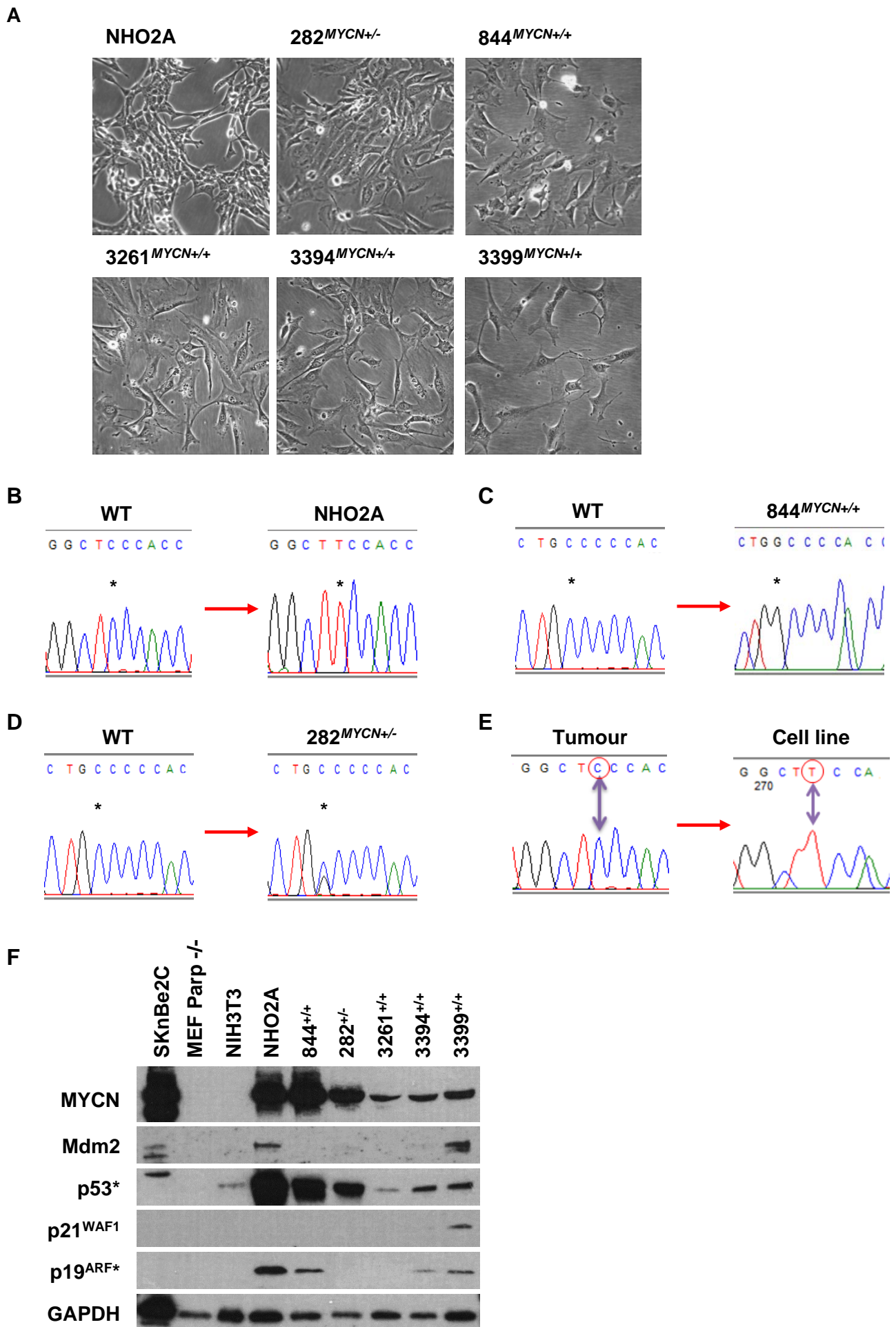
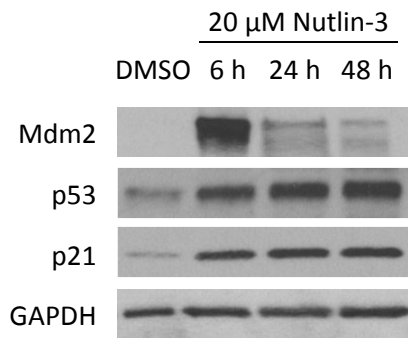
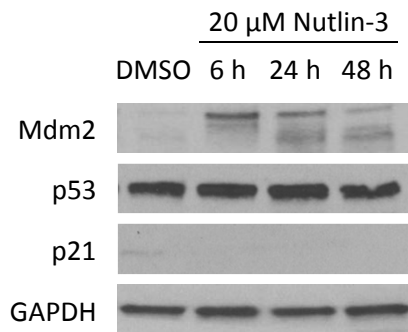


Figure 2

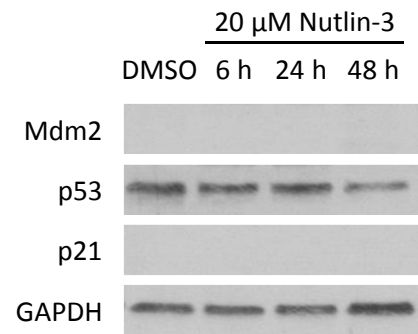
A **MEF^{PARP-/-}**



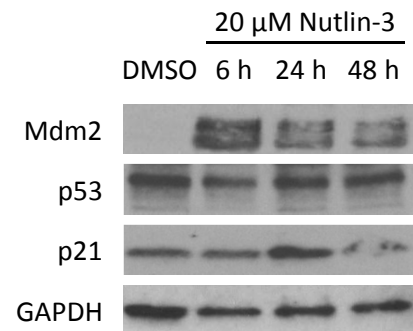
B **NHO2A**



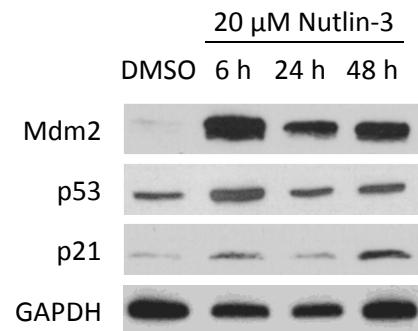
C **844^{MYCN+/+}**



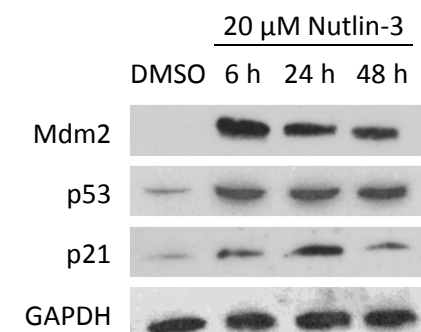
D **282^{MYCN+/-}**



E **3261^{MYCN+/+}**



F **3394^{MYCN+/+}**



G **3399^{MYCN+/+}**

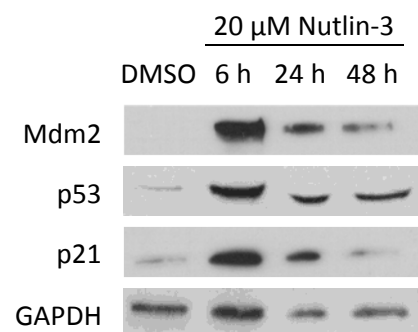
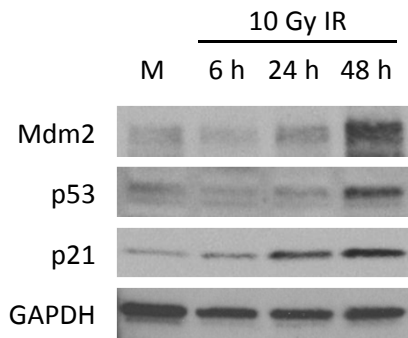
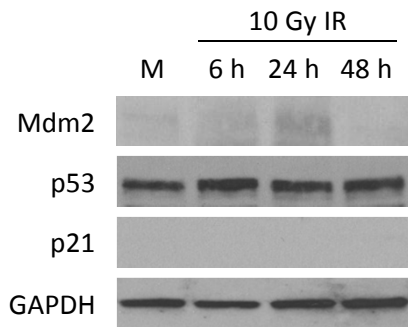


Figure 3

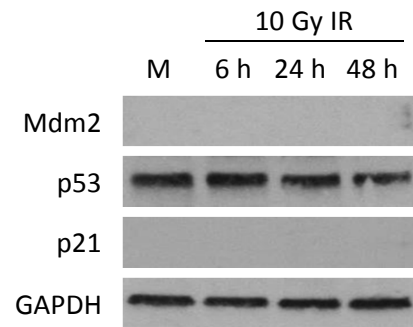
A MEF^{PARP-/-}



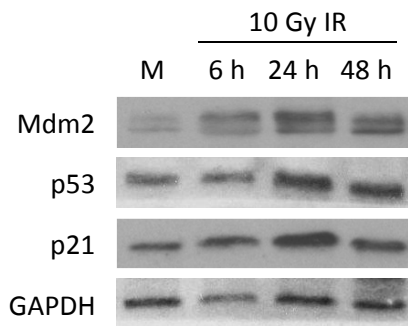
B NHO2A



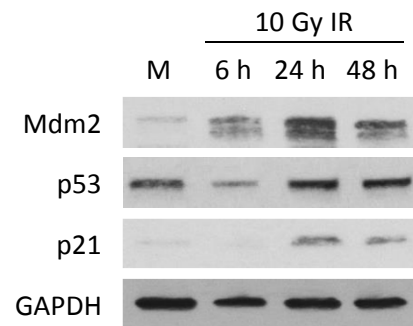
C 844^{MYCN+/+}



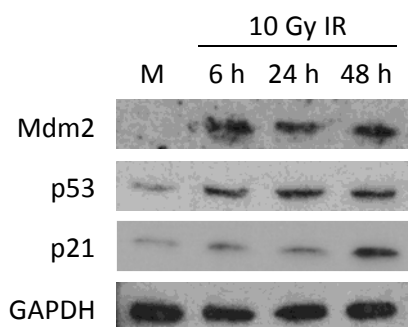
D 282^{MYCN+/-}



E 3261^{MYCN+/+}



F 3394^{MYCN+/+}



G 3399^{MYCN+/+}

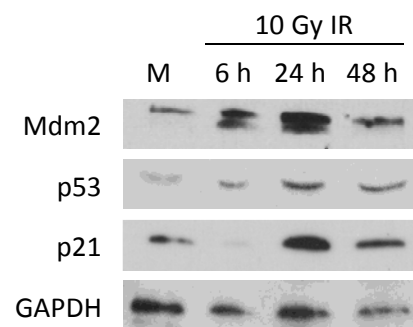
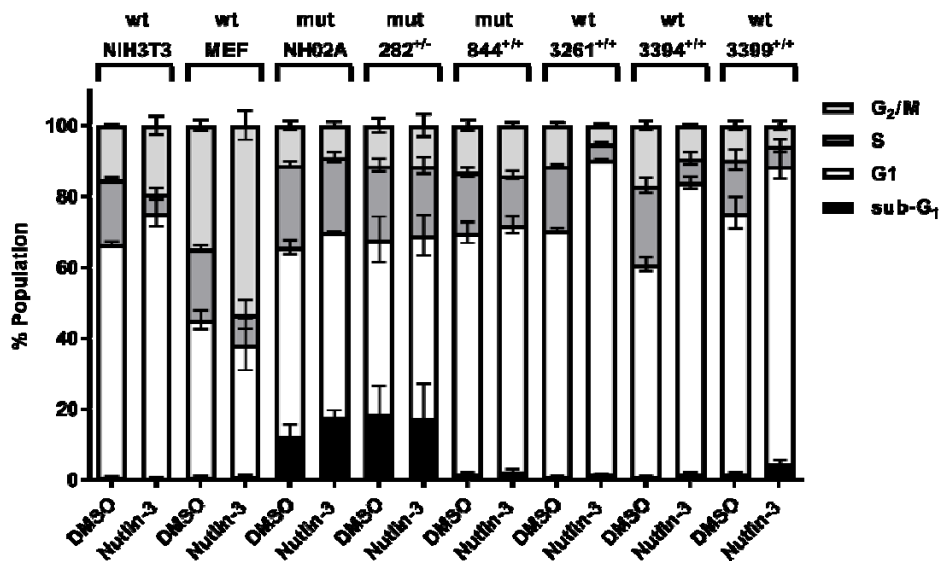
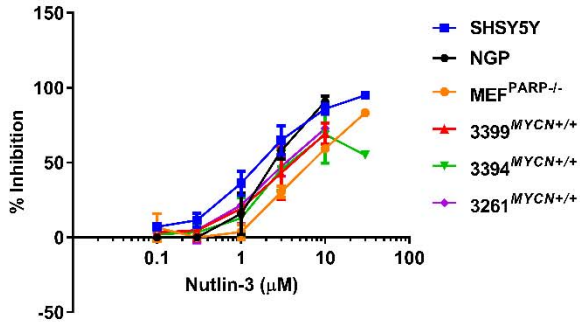


Figure 4

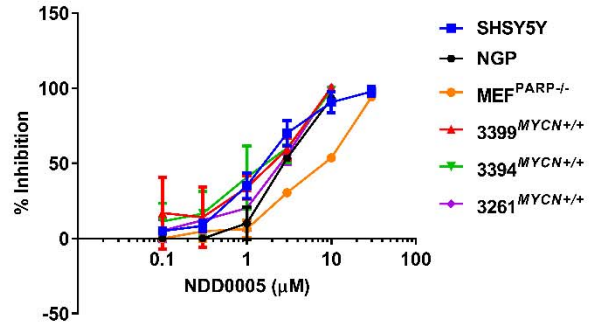
A



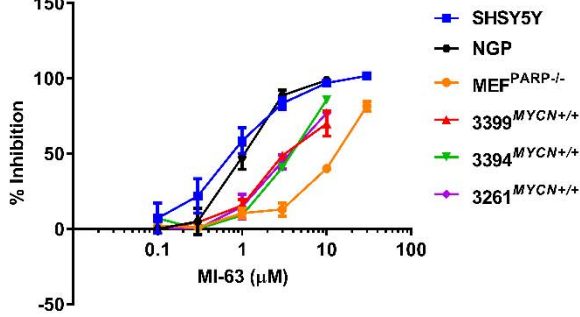
B



C



D



E

